1 Alignment Method

It's too late at night for me to write a proper document, so I'm just going to write enough here for you to understand what I'm doing. It will be the basis for a better write-up later.

The goal is to align as many degrees of freedom as possible using the information provided by residuals between tracks and hits. To get the most information out of a track's intersection with a chamber, we first combine all of its residuals into a super-residual which expresses the difference in position between the track and all of its hits and the difference in angle between the track and all of its hits. We compute this position difference and angle difference from an analytic linear fit, e.g. for Δx_i residuals on layers of fixed z_i,

$$\text{position difference} = a = \frac{1}{\text{denominator}}\left(\sum\frac{z_i^2}{\sigma_i^2}\sum\frac{\Delta x_i}{\sigma_i^2} - \sum\frac{z_i}{\sigma_i^2}\sum\frac{z_i\Delta x_i}{\sigma_i^2}\right) \quad (1)$$

$$\text{angle difference} = b = \frac{1}{\text{denominator}}\left(\sum\frac{1}{\sigma_i^2}\sum\frac{z_i\Delta x_i}{\sigma_i^2} - \sum\frac{z_i}{\sigma_i^2}\sum\frac{\Delta x_i}{\sigma_i^2}\right) \quad (2)$$

$$\text{where denominator} = \sum\frac{1}{\sigma_i^2}\sum\frac{z_i^2}{\sigma_i^2} - \left(\sum\frac{z_i}{\sigma_i^2}\right)^2 \quad (3)$$

$$\text{with } \chi^2/N_{\text{dof}} = \frac{1}{N_{\text{hits}}-2}\sum\frac{\Delta(x_i - a - z_i\,b)^2}{\sigma_i^2} \text{ as a quality parameter.} \quad (4)$$

Super-residuals are more precise than segment residuals because we only assume that the difference between the muon's path and the track's propagation is linear. The muon may be following a curved path, for example in ME1/1, where $|\vec{B}| > 2.5$ T.

(Editorial comment: I think this method provides more information than using the 1-D hits individually, because it inserts the information that the hits in the same chamber have smaller relative errors than hits in different chambers.)

DT chambers in stations 1, 2, and 3 are capable of measuring local x and y coordinates, while DT chambers in station 4 can measure only local x. CSC chambers can in principle measure x and y using intersections of cathode strips and anode wires, but the wires are ganged in 5 cm groups, which is too large of a granularity for alignment. (The chambers are already better aligned than that.) Moreover, the stips are not parallel, but fan radially from the beamline, so that they are directly sensitive to the curvilinear coordinate $r\phi$ rather than the cartesian x (Fig 1). To use the chamber's best information, we extract $r\phi$ residuals from the CSCs. Combining these residuals into super-residuals using the method of Eqn 4, we obtain

- Δx and Δy position super-residuals and $\Delta\frac{dx}{dz}$ and $\Delta\frac{dy}{dz}$ angular super-residuals from chambers in barrel stations 1, 2, and 3,
- Δx position and $\Delta\frac{dx}{dz}$ angular super-residuals from chambers in barrel station 4, and
- $\Delta r\phi$ position and $\Delta\frac{dr\phi}{dz}$ angular super-residuals from CSC chambers.

It is easy to see that an offset in Δx super-residuals is an indication of a δ_x misalignment, and with some geometry (Fig 2), relationships between the six alignment parameters (δ_x, δ_y, δ_z, δ_{ϕ_x}, δ_{ϕ_y}, and δ_{ϕ_z}) and the super-residuals can be derived. The complete set of relationships

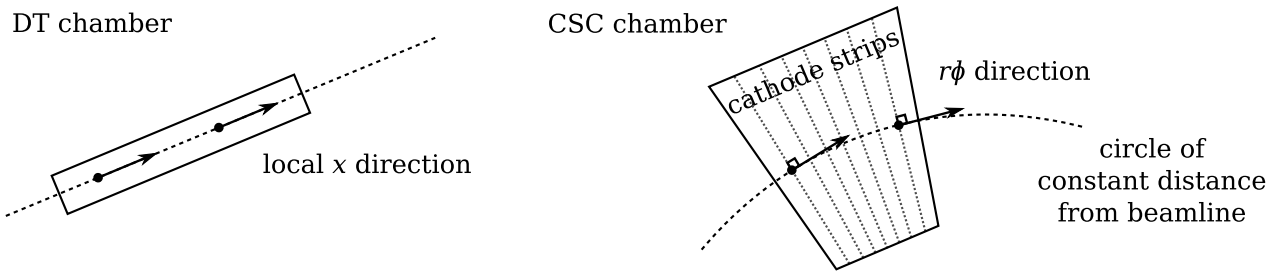

Figure 1: Local x and y coordinates in DT chambers are rectilinear, but the fanning of CSC strips makes it more convenient to measure residuals and align CSCs in curvilinear $r\phi$.

can be written as a matrix, expressing the geometric correction each alignment parameter imposes upon the residuals.

$$\begin{pmatrix} \Delta x^{\text{geom}} \\ \Delta y^{\text{geom}} \\ \Delta\frac{dx}{dz}^{\text{geom}} \\ \Delta\frac{dy}{dz}^{\text{geom}} \end{pmatrix} = \begin{pmatrix} 1 & 0 & -\frac{dx}{dz} & -y\frac{dx}{dz} & x\frac{dx}{dz} & -y \\ 0 & 1 & -\frac{dy}{dz} & -y\frac{dy}{dz} & x\frac{dy}{dz} & x \\ 0 & 0 & 0 & -\frac{dx}{dz}\frac{dy}{dz} & 1+\left(\frac{dx}{dz}\right)^2 & -\frac{dy}{dz} \\ 0 & 0 & 0 & -1-\left(\frac{dy}{dz}\right)^2 & \frac{dx}{dz}\frac{dy}{dz} & \frac{dx}{dz} \end{pmatrix} \begin{pmatrix} \delta_x \\ \delta_y \\ \delta_z \\ \delta_{\phi_x} \\ \delta_{\phi_y} \\ \delta_{\phi_z} \end{pmatrix} \tag{5}$$

where x, y, $\frac{dx}{dz}$, and $\frac{dy}{dz}$ denote the impact point and entrance angle of the track. The top two rows are the "Karimaki derivatives" used in the tracker to align all 6 degrees of freedom with two position residuals. The addition of super-residual angles $\Delta\frac{dx}{dz}$ and $\Delta\frac{dy}{dz}$ adds significance to δ_{ϕ_y} and δ_{ϕ_x} alignments, respectively, and all four observables contribute roughly equally to our determination of δ_{ϕ_z}.

In DT station 4, the lack of Δy and $\Delta\frac{dy}{dz}$ residuals reduces the relationship to a submatrix of the above, and δ_y cannot be aligned.

$$\begin{pmatrix} \Delta x^{\text{geom}} \\ \Delta\frac{dx}{dz}^{\text{geom}} \end{pmatrix} = \begin{pmatrix} 1 & 0 & -\frac{dx}{dz} & -y\frac{dx}{dz} & x\frac{dx}{dz} & -y \\ 0 & 0 & 0 & -\frac{dx}{dz}\frac{dy}{dz} & 1+\left(\frac{dx}{dz}\right)^2 & -\frac{dy}{dz} \end{pmatrix} \begin{pmatrix} \delta_x \\ \delta_y \\ \delta_z \\ \delta_{\phi_x} \\ \delta_{\phi_y} \\ \delta_{\phi_z} \end{pmatrix} \tag{6}$$

Though we treat CSCs as one-dimensional devices, the curvilinear coordinate modifies its matrix from the above. In principle, all 6 degrees of freedom are accessible to CSCs because strips near the edges of the trapezoidal chambers measure linearly independent combinations

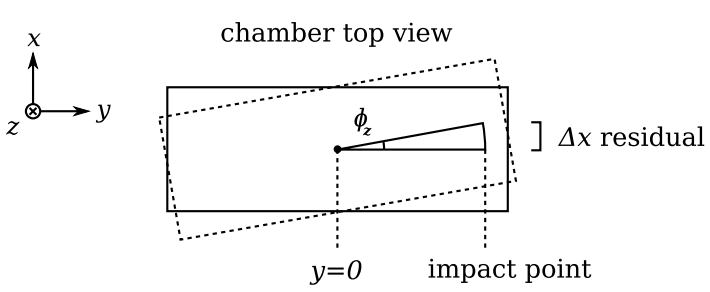

(a) Linear relationship between Δx residuals, $\delta\phi_z$ misalignment, and y track position: $\Delta x^{\text{geom}} = y\,\delta_{\phi_z}$

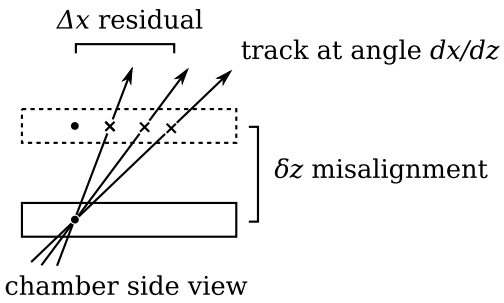

(b) Linear relationship between Δx residuals, δz misalignment, and dx/dz track angle: $\Delta x^{\text{geom}} = (dx/dz)\,\delta z$

Figure 2: Geometric arguments justifying two of the matrix elements in Eqn 5

of δ_x and δ_y. Here is the CSC matrix (keeping only important terms):

$$\begin{pmatrix} \Delta r\phi^{\text{geom}} \\ \Delta\dfrac{dr\phi}{dz}^{\text{geom}} \end{pmatrix} = \begin{pmatrix} 1 & \left[-\dfrac{x}{R} + 3\left(\dfrac{x}{R}\right)^3\right] & -\dfrac{dx}{dz} & -y\dfrac{dx}{dz} & x\dfrac{dx}{dz} & -y \\ 0 & -\dfrac{dx}{dz}/(2R) & 0 & \left[\dfrac{x}{R} - \dfrac{dx}{dz}\dfrac{dy}{dz}\right] & 1 + \left(\dfrac{dx}{dz}\right)^2 & -\dfrac{dy}{dz} \end{pmatrix} \begin{pmatrix} \delta_x \\ \delta_y \\ \delta_z \\ \delta_{\phi_x} \\ \delta_{\phi_y} \\ \delta_{\phi_z} \end{pmatrix} \tag{7}$$

where R is the distance to the convergence point of the strips, nominally the beamline *(and assumed to be the beamline in the current version of the code).*

Without measurement error, alignment would be a matter of solving Eqns 5–7 by matrix inversion. Five effects broaden the residuals distributions:

- statistical propagation error from the tracker: the track coordinates are not perfectly known, and errors in direction and curvature grow linearly and quadratically with arclength along the track, respectively,
- systematic misalignment error from the tracker, which might have a global pattern,
- multiple-scattering in material, which adds Gaussian statistical error independently to each track,
- single-scattering in material, which adds statistical error with a power-law distribution,
- and chamber detector resolution, which is statistical and smaller than the above.

All of the statistical errors (everything except tracker misalignment) can be expressed as a fit function. The fact that single scattering has a non-Gaussian distribution complicates the function somewhat, in that the distribution must be a convolution of a Gaussian with a bell curve with power-law tails: we choose a Lorentz-Cauchy distribution for convenience. The most important feature of the non-Gaussian part of the fit is its reduced sensitivity to outlying events.

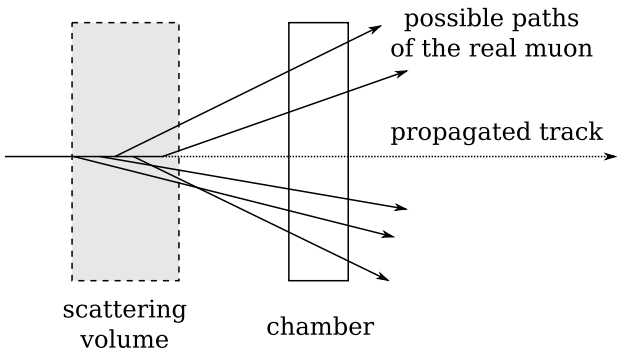

Figure 3: Correlation between super-residual position error and angle error.

There is also a strong correlation between position residuals and their corresponding angle residuals. Tracks reconstructed with the wrong direction for any reason (scattering, measurement error in the tracker) will tend to be offset in position when they reach the chamber by an amount proportional to the length of the track (see Fig 3). We can accommodate for this correlation by adding fit parameters α_x and α_y, for which

$$\Delta x^{\text{average}} = \alpha_x \, \Delta \frac{dx}{dz}^{\text{average}} \tag{8}$$

$$\Delta y^{\text{average}} = \alpha_y \, \Delta \frac{dy}{dz}^{\text{average}} \tag{9}$$

The fit function for a two-residual chamber such as DT station 4 and the CSCs is

$$f_x(\Delta x; \Delta x^{\text{geom}}, \alpha_x, \Delta \frac{dx}{dz}, \sigma_x, \gamma_x) = \int_{-\infty}^{\infty} \frac{\gamma_x}{\pi} \left(\left(\Delta x - \xi - \Delta x^{\text{geom}} - \alpha_x \, \Delta \frac{dx}{dz} \right)^2 + {\gamma_x}^2 \right)^{-1} \times \frac{1}{\sqrt{2\pi}\sigma_x} \exp\left(\frac{-\xi^2}{2{\sigma_x}^2} \right) d\xi \tag{10}$$

$$g_x(\Delta \frac{dx}{dz}; \Delta \frac{dx}{dz}^{\text{geom}}, \sigma_{\frac{dx}{dz}}, \gamma_{\frac{dx}{dz}}) = \int_{-\infty}^{\infty} \frac{\gamma_{\frac{dx}{dz}}}{\pi} \left(\left(\Delta \frac{dx}{dz} - \xi - \Delta \frac{dx}{dz}^{\text{geom}} \right)^2 + {\gamma_{\frac{dx}{dz}}}^2 \right)^{-1} \times \frac{1}{\sqrt{2\pi}\sigma_{\frac{dx}{dz}}} \exp\left(\frac{-\xi^2}{2{\sigma_{\frac{dx}{dz}}}^2} \right) d\xi \tag{11}$$

where we fit simultaneously for f_x and g_x, implicitly including all of the alignment parameters in Δx^{geom} and $\Delta \frac{dx}{dz}^{\text{geom}}$. DT chambers in stations 1, 2, and 3 are simultaneous fits for f_x, f_y, g_x, and g_y, where f_y and g_y are defined similarly to the above. The width parameters σ_x, $\sigma_{\frac{dx}{dz}}$, γ_x, and $\gamma_{\frac{dx}{dz}}$ are the Gaussian width and the Lorentzian half-width at half maximum (before convolution). We use MINUIT to fit the observed super-residuals to the above function in an unbinned maximum likelihood fit, weighted by the inverse of super-residual quality $(\chi^2/N_{\text{dof}})^{-1}$.

2 Progress

It was very important to include all alignment parameters for each chamber into a single fit. Excluding the $\Delta\frac{dx}{dz} = -\frac{dy}{dz}\,\delta_{\phi_z}$ matrix element caused the fits to not converge in random initial conditions, and an apparent confusion between ϕ_y and ϕ_z in more controlled initial conditions. On Wednesday, I was thinking of cobbling together a procedure which aligns parameters in a particular order to make this sensitivity irrelevant. By including it in the fit function, it now becomes a part of the measurement. I have verified that this works.

The tests of Eqns 5–7 were extensive. I discovered them via a mathematical model I made in Python (therefore I know exactly what went into the calculation), verified them in full CMSSW with the propagator intersecting alignable chamber surfaces (therefore I know that I got all of the sign conventions right), but without measurement error, and I have verified that ϕ_y and ϕ_z are properly decoupled in the full Monte Carlo. This method correctly derived the Karimaki part of the matrix (top two rows— a HIP algorithm without super-residual angles, like the one used in the tracker).

Trying to solve the fit-failure problem (below), I have tweaked the fit function to a very high degree. Weighting the super-residuals by $(\chi^2/N_{\mathrm{dof}})^{-1}$ has cleaned up the shape considerably. Consistency of hits with a straight line is a geometric property, unlike hit uncertainty which can sometimes be ad-hoc and describe Monte Carlo much better than data, so these weights are unlikly to cause problems in data.

Still trying to solve the fit-failures, I also improved the numerical stability of the fit function. Convolutions are computationally expensive, so it must be tabulated, with points between the table entries computed by interpolation. Rather than tabulate $f((x-x_0)/\sigma,\ \gamma/\sigma)$, I tabulated $\log f((x-x_0)/\sigma,\ \gamma/\sigma)$, interpolate in the log space, and pass this to MINUIT as the log likelihood. I also made the binning ten times smaller in γ/σ. Outside of the table ($\gamma/\sigma > 5$ and $(x-x_0)/\sigma > 50$) is now represented by a pure Lorentzian, as that is what the curve limits to at those extremes. The transition from the table to pure Lorentzian is relatively smooth, and most distributions have $\gamma/\sigma \approx 0.1$.

3 Problems

Many of the fits fail in MINUIT. This problem has become more frequent now that more parameters have been added to the fit, and MINUIT's most frequent error messages are "Hessian not positive definite," and "Machine precision isn't good enough to verify convergence" (implying a very shallow or a very non-smooth minimum). However, this is still an issue when many of the parameters are fixed at reasonable values (verified by plotting). Fits are always given reasonable starting values, computed from carefully truncated means and standard deviations, and even a linear pre-fit to seed the largest correlation (between Δy and $\Delta\frac{dy}{dz}$). The problem also seems to be independent of whether the parameters are given reasonable limits or not. By default, I don't assign limits.

An important clue comes from the fact that replacing the fit function (Eqns 10-11) with pure Gaussian distributions always fits successfully (after $\log(\exp(-x^2))$ was replaced by $-x^2$). Unfortunately, the distributions are not well described by Gaussians, and this can seriously deteriorate the alignment results. (Gaussian widths are ∼10-100 mm. The

only way to get a good measurement of the peak position is to do a very precise fit of the distribution.) That's why I revisited the formulation of the fit function, to make sure that it is smooth.

Successful fits are a little disappointing, too: the alignment results differ from MC truth by 3–5 standard deviations. The geometry matricies (Eqns 5–7) are definitely not at fault, because they perform perfectly in the absence of measurement error. I suspect that whatever is causing the fit failures (now about 50%) is deteriorating the quality of the successful fits—that's why I now consider this an important issue.

If there's a robust way to find the maximum likelihood of the full fit function without MINUIT, I'm willing to try it. Scanning probably won't work: the search space has too many dimensions for this to be feasible.

A less important issue is that strict proportionality between Δx and $\Delta\frac{dx}{dz}$ and between Δy and $\Delta\frac{dy}{dz}$ doesn't model the data well. The central region ($|\Delta\frac{dx}{dz}| < 5$ mrad and $|\Delta\frac{dy}{dz}| <$ 30 mrad, about 1 standard deviation in each) is linear, but outside of the is uncorrelated, so the whole distribution has more of an S-shape. 2-d distributions and ntuple exploration doesn't reveal why this is so. It doesn't seem to be related to the fit failures, but it might be important because this is the largest correlation, larger than any alignment correlation.